American Mineralogist, Volume 84, pages 1370–1374, 1999

Thermodynamics of cation ordering in karrooite ($MgTi_2O_5$)

MARK S. GHIORSO,[1,*] HEXIONG YANG,[2] AND ROBERT M. HAZEN[2]

[1]Department of Geological Sciences, Box 351310, University of Washington, Seattle, Washington 98195-1310, U.S.A.
[2]Geophysical Laboratory and Center for High Pressure Research, Carnegie Institution of Washington, 5251 Broad Branch Road, N.W., Washington, D.C., 20015-1305, U.S.A.

ABSTRACT

A thermodynamic model of non-convergent cation-ordering in karrooite ($MgTi_2O_5$) has been calibrated from the single-crystal X-ray structure refinements of Yang and Hazen (1998) and from estimates of the dependence of the bulk modulus on ordering state (Hazen and Yang 1997). Derived values of the Gibbs free energy, enthalpy, entropy, and heat capacity of disordering of karrooite are reported as a function of temperature at 1 bar and at elevated pressures.

INTRODUCTION

In this paper we develop a thermodynamic model that describes cation ordering as a function of temperature and pressure in the karrooite ($MgTi_2O_5$) end-member of the armacolite solid-solution series. The model is constructed utilizing techniques first developed by Thompson (1969, 1970) to describe cation order-disorder phenomena in minerals in terms of the principle of homogeneous equilibrium. The present study was prompted by the recent completion (Yang and Hazen 1998) of high quality, one-atmosphere X-ray structure refinements of single crystals of synthetic karrooite, which were equilibrated prior to analysis at temperatures over the range 600–1400 °C. The results of the study of Yang and Hazen (1998) are at odds with previous estimates of the equilibrium ordering state of karrooite (especially at elevated temperatures) and, consequently, existing formulations of the thermodynamics of cation ordering in this phase (Brown and Navrotsky 1989) require reevaluation in light of the recent results. We take this opportunity to develop a thermodynamic model that accounts for the Yang and Hazen (1998) measurements, and incorporate into the formulation a pressure dependence of this cation-ordering phenomena by accounting for the effect of ordering on the compressibility estimates of Hazen and Yang (1997).

THERMODYNAMIC ANALYSIS

A description of the karrooite structure and its relationship to other pseudobrookite-type oxide solid solutions is summarized by Waychunas (1991). For the present purpose, it is sufficient to understand that the Mg^{2+} and Ti^{4+} cations are distributed over two types of octahedral sites, M1 and M2, which are present in the ratio 1:2, respectively. The cation ordering, which is consequently of non-convergent type, therefore can be quantified by inventorying the proportion of Mg^{2+} or Ti^{4+} occupying either site. We may define an ordering parameter, s, to accomplish this task:

$$s = X_{Mg}^{M1} - 2X_{Mg}^{M2} \tag{1}$$

where X_{Mg}^{M1} denotes the mole fraction of Mg^{2+} on the M1 octahedral site and X_{Mg}^{M2} denotes the mole fraction of Mg^{2+} on the M2 octahedral site. The experimental evidence demonstrates that s is a function of both temperature and pressure. Note that the order parameter defined in Equation 1 is different from that adopted by Brown and Navrotsky (1989) or by Yang and Hazen (1998). Our choice is motivated by a desire to simplify the thermodynamic treatment by generating an order parameter that assumes values over the range 1 to –1 in proceeding from the fully ordered ($X_{Mg}^{M1} = 1$, $X_{Mg}^{M2} = 0$; $s = 1$) to the fully antiordered ($X_{Mg}^{M1} = 0$, $X_{Mg}^{M2} = 1/2$; $s = -1$) state. The algebraic simplification with this definition is considerable. It should also be noted that a random cation configuration is given by $X_{Mg}^{M1} = X_{Mg}^{M2} = 1/3$; $s = -1/3$. From Equation 1 it follows that:

$$X_{Mg}^{M1} = \frac{1+s}{2} \tag{2a}$$

$$X_{Mg}^{M2} = \frac{1-s}{4} \tag{2b}$$

$$X_{Ti}^{M1} = \frac{1-s}{2} \tag{2c}$$

and

$$X_{Ti}^{M2} = \frac{3+s}{4}. \tag{2d}$$

The configurational entropy ($\bar{S}^{conf}$) associated with the degree of cation order is:

$$\bar{S}^{conf} = -R\left(X_{Mg}^{M1}\ln X_{Mg}^{M1} + X_{Ti}^{M1}\ln X_{Ti}^{M1} + 2X_{Mg}^{M2}\ln X_{Mg}^{M2} + 2X_{Ti}^{M2}\ln X_{Ti}^{M2}\right) \tag{3}$$

which, via Equations 2a–d may be written as a function solely of the order parameter, s:

$$\bar{S}^{conf} = -R\left(\frac{1+s}{2}\ln\frac{1+s}{2} + \frac{1-s}{2}\ln\frac{1-s}{2} + \frac{1-s}{2}\ln\frac{1-s}{4} + \frac{3+s}{2}\ln\frac{3+s}{4}\right) \tag{4}$$

We construct a thermodynamic model for karrooite ordering by writing an expression for the molar Gibbs free energy ($\bar{G}$) of the phase in terms of configurational ($-T\bar{S}^{conf}$) and lattice vibrational ($\bar{G}^{*}$) contributions:

*E-mail: ghiorso@u.washington.edu

$$\bar{G} = -T\bar{S}^{\text{conf}} + \bar{G}^{*} \tag{5}$$

taking the vibrational component to be a second-order truncated Taylor expansion in the order parameter:

$$\bar{G}^{*} = \bar{G}^{*}_{0} + \bar{G}^{*}_{s}s + \bar{G}^{*}_{s2}s^{2}. \tag{6}$$

The Taylor coefficients in Equation 6, $\bar{G}^{*}_{0}$, $\bar{G}^{*}_{s}$, and $\bar{G}^{*}_{s2}$, are conveniently recast in terms of more intuitive energetic quantities. Adopting $\bar{G}^{0}_{\text{Kar}}$ to denote the molar Gibbs free energy of fully ordered karrooite ($Mg^{M1}Ti_2^{M2}O_5$) at any T and P, along with $\Delta\bar{G}^{0}_{\text{EX}}$ to describe the free energy change of the ordering reaction:

$$Mg^{M1}Ti_2^{M2}O_5 = Ti^{M1}(Mg,Ti)_2^{M2}O_5 \tag{7}$$

and W_G to refer to a "regular solution type" parameter defining the non-linearity of the Gibbs energy along the $Mg^{M1}Ti_2^{M2}O_5$-$Ti^{M1}(Mg,Ti)_2^{M2}O_5$ join, Equation 6 may be transformed into

$$\bar{G}^{*} = \bar{G}^{0}_{\text{Kar}} + \frac{1}{2}\Delta\bar{G}^{0}_{\text{EX}}(1-s) + \frac{1}{4}W_G(1-s^2). \tag{8}$$

Equations 4, 5, and 8 define our thermodynamic model. In general, the model parameters $\Delta\bar{G}^{0}_{\text{EX}}$ and W_G may be functions of *both temperature and pressure*. First-order expansions in both T and P are adopted for preliminary analysis of the experimental data sets:

$$\Delta\bar{G}^{0}_{\text{EX}} = \Delta\bar{H}^{0}_{\text{EX}} - T\Delta\bar{S}^{0}_{\text{EX}} + \Delta\bar{V}^{0}_{\text{EX}}(P-1), \tag{9}$$

$$W_G = W_H - TW_S + W_V(P-1). \tag{10}$$

Experimental measurements of ordering state in karrooite as a function of T and P provide a means of calibrating $s(T,P)$ under the assumption that the measurements reflect an "equilibrium" state of cation order. In thermodynamic equilibrium, the molar Gibbs free energy is minimal with variation in s at fixed T and P:

$$\frac{\partial\bar{G}}{\partial s} = 0 \tag{11}$$

which from Equations 4, 5, 8, 9, and 10, results in:

$$RT\left[\ln\frac{(1+s)(3+s)}{(1-s)^2}\right] = \Delta\bar{H}^{0}_{\text{EX}} - T\Delta\bar{S}^{0}_{\text{EX}} + (P-1)\Delta\bar{V}^{0}_{\text{EX}} + \left[W_H - TW_S + (P-1)W_V\right]s. \tag{12}$$

The model parameters in Equation 12, e.g., $\Delta\bar{H}^{0}_{\text{EX}}$, $\Delta\bar{S}^{0}_{\text{EX}}$, $\Delta\bar{V}^{0}_{\text{EX}}$, W_H, W_S, and W_V, must be calibrated from experimental data.

In Figure 1 we plot values of

$$RT\ln\left[\frac{(1+s)(3+s)}{(1-s)^2}\right]$$

as a function of s, derived from the measurements of Yang and Hazen (1998). The data point labeled 600° C is problematic. The karrooite samples Yang and Hazen (1998) utilized for their analysis were prepared from synthetic oxides at high temperatures (1200 °C). Single crystals were then selected and annealed at the temperatures indicated in Figure 1. In the case of the 600 °C sample, an annealing time of 1008 hours was probably insufficient; repeated analysis of crystals "equilibrated" at this temperature demonstrated inconsistent values of lattice constants. For this reason, in the subsequent calibration of our model from these data we will utilize the 600 °C measurement for reference and not constrain the model to fit this datum.

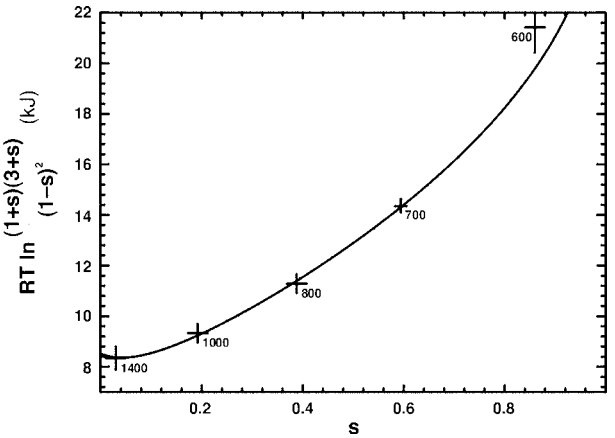

FIGURE 1. Analysis of Cation-ordering data for Karrooite according to Equation 12 (see text). Measurements of Yang and Hazen (1998) are plotted with 2σ uncertainties and are labeled with the temperature (°C) of annealing. s is given by Equation 1. The solid curve is the model representation of the data.

As the Yang and Hazen (1998) data were collected at a pressure of 1 bar, the array of points should be modeled according to (e.g., Eq. 12):

$$RT\left[\ln\frac{(1+s)(3+s)}{(1-s)^2}\right] = \Delta\bar{H}^{0}_{\text{EX}} - T\Delta\bar{S}^{0}_{\text{EX}} + \left[W_H - TW_S\right]s \tag{12'}$$

Extensive studies of numerous oxide (Ghiorso 1990a; Sack and Ghiorso 1991a, 1991b) and silicate (Ghiorso et al. 1995; Hirschmann and Ghiorso 1994; Sack and Ghiorso 1989, 1994a, 1994b, 1994c, 1998) mineral solid solutions have demonstrated that excess vibrational entropies (i.e., non-zero values of $\Delta\bar{S}^{0}_{\text{EX}}$ or W_S) are never required to model cation order-disorder phenomena unless there is a strong disparity in the effect of temperature on the coordination number or geometry of one site over the other (e.g., pigeonite → high Ca-pyroxene, Sack and Ghiorso 1994b). Such is the case in karrooite (Brown and Navrotsky 1989; Yang and Hazen 1998), and the consequences can be seen in the intrinsic curvature of the array of points plotted in Figure 1. Even if the 1400 °C point is removed from consideration, on the argument that the highest temperature equilibrium ordering state may be unquenchable, the curvature is still apparent and outside the 2σ uncertainty of the three points at 1000, 800, and 700 °C. In the context of our model expression (Eq. 12'), this curvature can be accounted for by varying either the slope of the curve as a function of T (non-zero W_S) or the intercept (non-zero $\Delta\bar{S}^{0}_{\text{EX}}$) or both. Least-squares analysis of these three possibilities, utilizing maximal F-value as an optimality criteria (Daniel and Wood 1980), indicates a parameterization with $\Delta\bar{S}^{0}_{\text{EX}}$ set to zero is the best choice. The resulting values for $\Delta\bar{H}^{0}_{\text{EX}}$, W_H, and W_S are provided in Table 1. The model curve is plotted in Figure 1.

In Figure 2, we plot s as a function of T showing our model prediction and indicating the measurements of Yang and Hazen (1998) and the inferences of Brown and Navrotsky (1989). Ordering state estimates derived from the latter study were not obtained from single crystal structure refinements and consequently are not to be regarded with the same weight as the data

TABLE 1. Suggested model parameters

Model parameter	Value	
$\Delta\overline{H}^0_{EX}$	17.0177	(kJ)
$\Delta\overline{S}^0_{EX}$	0	
$\Delta\overline{V}^0_{EX}$	0	
W_H	59.3557	(kJ)
W_S	41.0611	(J/K)
W_V	0.0734607	(J/bar)
$\overline{V}^0_{Kar,0}$	5.46085	(J/bar)
$\overline{V}^0_{Kar,T}$	$8.25432\ 10^{-6}$	(J/bar-K)
$\overline{V}^0_{Kar,P}$	$-3.10675\ 10^{-6}$	(J/bar^2)
$\overline{V}^0_{Kar,T,P}$	$-2.0\ 10^{-10}$	($J/bar\text{-}K^2$)

Note: $\overline{V}^0_{Kar} = \overline{V}^0_{Kar,0} + \overline{V}^0_{Kar,T}\,T + \overline{V}^0_{Kar,P}(P-1) + \overline{V}^0_{Kar,T,P}(P-1)$

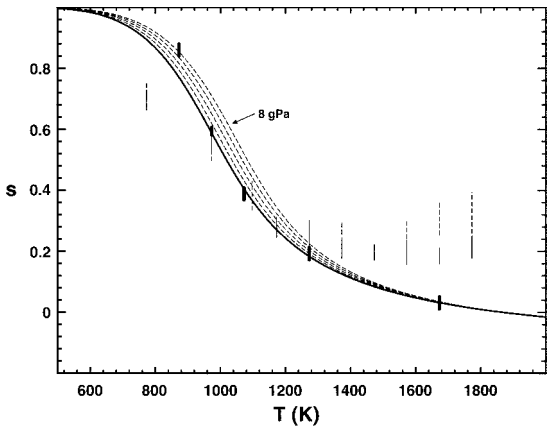

FIGURE 2. Ordering parameter (*s*) plotted as a function of temperature (*T*) for Karrooite. Heavy vertical black lines represent data of Yang and Hazen (1998) with two sigma uncertainties in *s*. Data plotted as thin solid and dashed vertical lines represent inferences of ordering state calculated by Brown and Navrotsky (1989) from high-temperature lattice parameter data. The solid curve is the model representation of the data at 1 bar pressure. Dashed curves are model isobars at pressures of 2, 4, 6, and 8 GPa (only the 8 GPa curve is labeled).

of Yang and Hazen (1998). The greatest disparity between the two sets of measurements arises at elevated temperature and most likely reflects difficulties associated with quenching of samples.

Having established a model for the variation of the order parameter with temperature at 1 bar pressure, we next turn to measurements of molar volume and compressibility in order to calibrate the remaining model parameters. From the definition of the total derivative of $\overline{G}$:

$$\mathrm{d}\overline{G} = \frac{\partial\overline{G}}{\partial s}\mathrm{d}s + \frac{\partial\overline{G}}{\partial T}\mathrm{d}T + \frac{\partial\overline{G}}{\partial P}\mathrm{d}P \tag{13}$$

we obtain a general expression for $\overline{V}$ ($\frac{\mathrm{d}\overline{G}}{\mathrm{d}P}$ at constant *T*),

$$\overline{V} = \frac{\partial\overline{G}}{\partial s}\frac{\mathrm{d}s}{\mathrm{d}P} + \frac{\partial\overline{G}}{\partial P} \tag{14}$$

which for the special case of equilibrium cation order ($\frac{\mathrm{d}\overline{G}}{\mathrm{d}s} = 0$), simplifies to:

$$\overline{V} = \frac{\partial\overline{G}}{\partial P}. \tag{15}$$

Differentiating our model expression for $\overline{G}$ according to Equation 15 yields:

$$\overline{V} = \overline{V}^0_{Kar} + \frac{1}{2}\Delta\overline{V}^0_{EX}(1-s) + \frac{1}{4}W_V(1-s^2). \tag{16}$$

The compressibility (β) is the inverse of the bulk modulus (K) and is defined in terms of the isothermal pressure derivative of the volume:

$$\beta = -\frac{1}{\overline{V}}\frac{\partial\overline{V}}{\partial P}. \tag{17}$$

To obtain a model expression for the compressibility, we take the derivative of Equation 14 with respect to pressure at constant temperature:

$$\frac{\partial\overline{V}}{\partial P} = \frac{\partial\overline{G}}{\partial s}\frac{\mathrm{d}^2 s}{\mathrm{d}P^2} + \frac{\partial^2\overline{G}}{\partial s^2}\left(\frac{\mathrm{d}s}{\mathrm{d}P}\right)^2 + 2\frac{\partial^2\overline{G}}{\partial s\partial P}\frac{\mathrm{d}s}{\mathrm{d}P} + \frac{\partial^2\overline{G}}{\partial P^2}. \tag{18}$$

The first term on the right hand side of Equation 18 vanishes in the special case of equilibrium cation order, but the next two terms do not! They represent the change of volume with respect to pressure induced changes in the ordering state. The partial derivatives of $\overline{G}$ are easily evaluated from our model expression:

$$\frac{\partial^2\overline{G}}{\partial s^2} = \frac{\mathrm{R}T(5+3s)}{(1+s)(1-s)(3+s)} - \frac{1}{2}W_G \tag{19}$$

$$\frac{\partial^2\overline{G}}{\partial s\partial P} = -\frac{1}{2}\Delta\overline{V}^0_{EX} - \frac{1}{2}W_V s \tag{20}$$

and

$$\frac{\partial^2\overline{G}}{\partial P^2} = -\frac{\partial\overline{V}^0_{Kar}}{\partial P}. \tag{21}$$

The variation of the order parameter with pressure *in an equilibrium state of cation order* can be obtained utilizing the method of Ghiorso (1990b). As $\frac{\partial\overline{G}}{\partial s} = 0$ in a state of equilibrium order, the total derivative of $\frac{\partial\overline{G}}{\partial s}$ must also be zero:

$$\mathrm{d}\left(\frac{\partial\overline{G}}{\partial s}\right) = 0 = \frac{\partial^2\overline{G}}{\partial s^2}\mathrm{d}s + \frac{\partial^2\overline{G}}{\partial s\partial T}\mathrm{d}T + \frac{\partial^2\overline{G}}{\partial s\partial P}\mathrm{d}P \tag{22}$$

from which at constant temperature:

$$\frac{\mathrm{d}s}{\mathrm{d}P} = -\frac{\partial^2\overline{G}}{\partial s\partial P}\Big/\frac{\partial^2\overline{G}}{\partial s^2}. \tag{23}$$

Substituting the definition in Equation 23 into Equation 18, gives the pressure dependence of the volume in an equilibrium state of cation order:

$$\frac{\partial\overline{V}}{\partial P} = -\left(\frac{\partial^2\overline{G}}{\partial s\partial P}\right)^2\Big/\frac{\partial^2\overline{G}}{\partial s^2} + \frac{\partial^2\overline{G}}{\partial P^2}. \tag{24}$$

Substitution of Equations 19, 20, and 21 relates this expression back to our adopted model parameters.

In Figure 3 we plot measured molar volumes of karrooite from Yang and Hazen (1998) as a function of ordering state (a) and temperature (b). In addition to these data, isothermal bulk moduli for this phase are plotted in Figure 4 as a function of temperature. These estimates are from the analysis of Hazen and Yang (1997) and are based on diamond-anvil cell experi-

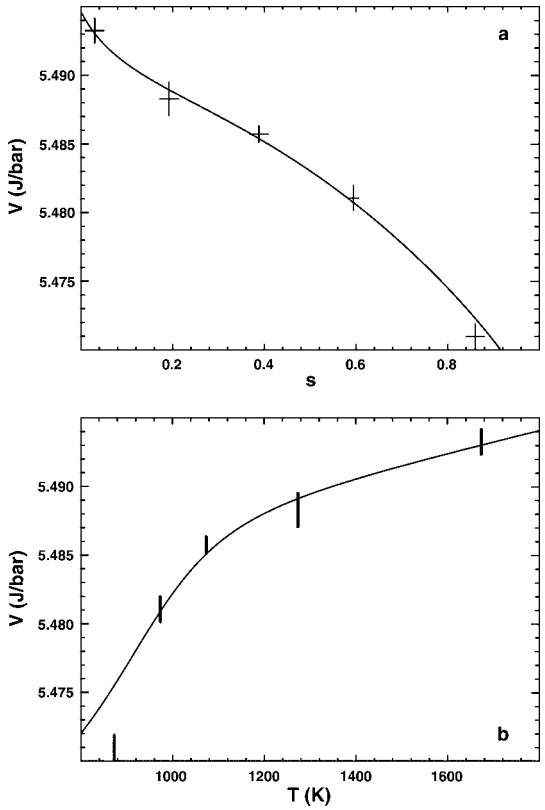

FIGURE 3. Volume (*V*) plotted against ordering parameter (*s*) in **a** and against temperature (*T*) in **b**. Data are from Yang and Hazen (1998) shown with 2σ uncertainties. The solid curves are the model representations of the data.

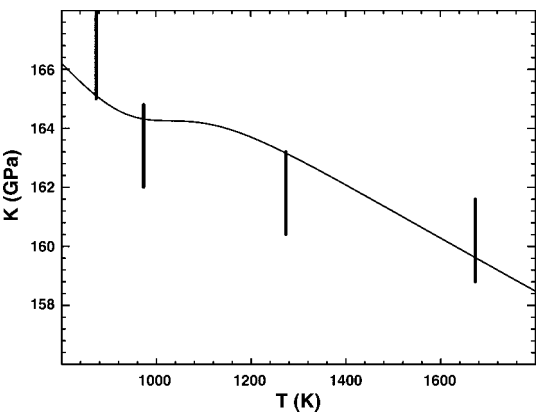

FIGURE 4. Bulk modulus (*K*) plotted against temperature (*T*). Estimated values are from Hazen and Yang (1997) shown with 2σ uncertainties. The solid curve is the model representation of the data.

ments on synthetic single crystals annealed at the indicated temperatures and quenched to room temperature. Both of these datasets are fitted to the proposed model simultaneously; for reasons outlined above, the 600 °C volume determinations were afforded zero weight. The resulting model curves are plotted on both figures and the optimal model parameter values are provided in Table 1.

DISCUSSION

The volume change associated with disordering the cation distribution in karrooite is given by $\overline{V} - \overline{V}(s\rightarrow 1)$:

$$\Delta\overline{V}^{\text{dis}} = \frac{1}{2}\Delta\overline{V}^{0}_{\text{EX}}(1-s) + \frac{1}{4}W_v\left(1-s^2\right). \tag{25}$$

Substitution of parameter values from Table 1 demonstrates that the right-hand side of Equation 25 is always positive, thereby implying that the Gibbs free energy of the disordered structure is always more positive than the ordered structure at a given temperature as pressure is increased. Consequently, there is a thermodynamic driving force for karrooite to become more ordered as pressure is increased at constant temperature. This effect can be quantified by calculating the variation in ordering state as a function of temperature at various pressures. Curves depicting this variation at a total pressure of 2, 4, 6, and 8 GPa are plotted in Figure 2. One interesting aspect to these calculations is that the effect of *P* on *s* appears to be maximized at intermediate temperatures. The maximum response corresponds to the point of inflection in the 1 bar *T*-*s* curve of Figure 2. We examine this aspect of the dependence of *s* on *P* in more detail in Figure 5. Here the derivative,

$$\frac{\mathrm{d}s}{\mathrm{d}P} = \frac{\frac{1}{2}\Delta\overline{V}^{0}_{\text{EX}} + \frac{1}{2}W_V s}{\frac{RT(5+3s)}{(1+s)(1-s)(3+s)} - \frac{1}{2}\left[W_H - TW_S + (P-1)W_V\right]} \tag{26}$$

(see above) is evaluated at a pressure of 1 bar and is plotted as a function of temperature. The maximum in d*s*/d*P*, seen at a temperature of around 1000 K, confirms the inference drawn from the spacing of the isobars in Figure 2. The calculation displayed in Figure 5 also illustrates a general feature about the thermodynamic response to non-convergent cation ordering phenomena: maximal temperature-variation in thermodynamic properties is observed at a temperature that corresponds to the maximal rate of change in *s*. This principle is best illustrated for karrooite by calculating as a function of temperature the Gibbs free energy, entropy, enthalpy, and heat capacity of disorder: $\Delta\overline{G}^{\text{dis}}$, $\Delta\overline{S}^{\text{dis}}$, $\Delta\overline{H}^{\text{dis}}$, and $\Delta\overline{C}_P^{\text{dis}}$ respectively. These quantities are defined analogously to Equation 25 and are given by:

$$\Delta\overline{G}^{\text{dis}} = -T\overline{S}^{\text{conf}} + \frac{1}{2}\Delta\overline{G}^{0}_{\text{EX}}(1-s) + \frac{1}{4}W_G\left(1-s^2\right) \tag{27}$$

$$\Delta\overline{S}^{\text{dis}} = \overline{S}^{\text{conf}} + \frac{1}{2}\Delta\overline{S}^{0}_{\text{EX}}(1-s) + \frac{1}{4}W_S\left(1-s^2\right) \tag{28}$$

$$\Delta\overline{H}^{\text{dis}} = \frac{1}{2}\Delta\overline{H}^{0}_{\text{EX}}(1-s) + \frac{1}{4}W_H\left(1-s^2\right) \tag{29}$$

and

$$\Delta\overline{C}_P^{\text{dis}} = T\left(\frac{\partial^2\overline{G}}{\partial s\,\partial T}\right)^2 \Big/ \frac{\partial^2\overline{G}}{\partial s^2} \tag{30}$$

where the later follows from an expression for the molar heat capacity,

$$\overline{C}_P = T\left(\frac{\partial^2\overline{G}}{\partial s\,\partial T}\right)^2 \Big/ \frac{\partial^2\overline{G}}{\partial s^2} - T\frac{\partial^2\overline{G}}{\partial T^2} \tag{31}$$

which may be derived in a fashion identical to Equation 24. Curves depicting the temperature dependence of $\Delta\overline{G}^{\text{dis}}$, $\Delta\overline{S}^{\text{dis}}$,

$\Delta\bar{H}^{dis}$, and $\Delta\bar{C}_P^{dis}$ at 1 bar and $\Delta\bar{G}^{dis}$ at 8 GPa are plotted in Figure 6. Note that the maximum in $\Delta\bar{C}_P^{dis}$ of ~55 J/K-mol at ~950 K is roughly 30% of the total heat capacity of karrooite at this temperature (Berman and Brown 1985). Note also the sympathetic variation of $\Delta\bar{S}^{dis}$ and $\Delta\bar{H}^{dis}$ and how this variation is to a certain extent, moderated by cancellation in $\Delta\bar{G}^{dis}$.

The thermodynamic analysis of cation-ordering in karrooite developed in this paper could be improved if "in situ" high-temperature cation-ordering data were available. The assumption that the measurements of Yang and Hazen (1998) represent quenched "equilibrium" states of order needs verification as the kinetics of ordering may be rapid enough, especially at high-T, to introduce systematic bias in the calibration. Nevertheless, the model formulation developed in this paper can be readily applied to the isostructural $FeTi_2O_5$ (known as ferro-pseudobrookite) and, in principle, can be extended to armacolite (Fe^{2+}-Mg) solid solutions, and more oxidized varieties of pseudobrookites (in the system $MgTi_2O_5$-$FeTi_2O_5$-Fe_2TiO_5) found in some alkalic volcanic rocks. What is required to extend the present analysis to these compositions is data on cation-ordering of a quality comparable to that of Yang and Hazen (1998). As demonstrated in this paper, these data provide all the essential information to define an equation of state for the phase that includes the important effects of cation order-disorder.

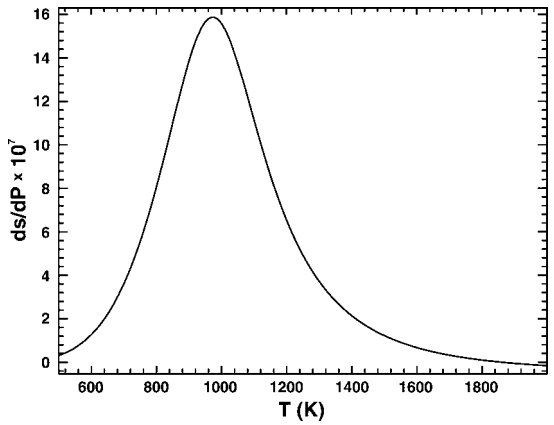

FIGURE 5. The rate of change of ordering parameter (s) with respect to pressure (P) plotted against temperature (T). The modeled curve (Eq. 26) displays a maximum at ~700 °C.

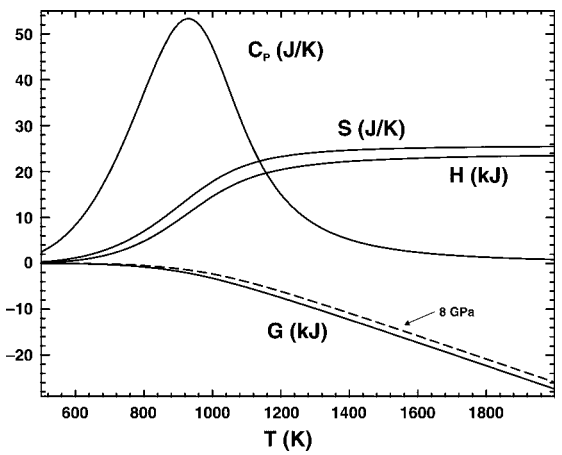

FIGURE 6. Calculated variation of the Gibbs free energy ($\Delta\bar{G}^{dis}$), entropy ($\Delta\bar{S}^{dis}$), enthalpy ($\Delta\bar{H}^{dis}$), and heat capacity ($\Delta\bar{C}_P^{dis}$) of disorder plotted as a function of temperature (T). The solid curves correspond to a pressure of 1 bar. The dashed curve show variation in $\Delta\bar{G}^{dis}$ at a pressure of 8 GPa.

ACKNOWLEDGMENTS

Material support for this investigation was provided to MSG by the National Science Foundation (OCE-9529790).

REFERENCES CITED

Berman, R.G. and Brown, T.H. (1985) Heat capacity of minerals in the system Na_2O-K_2O-CaO-MgO-FeO-Fe_2O_3-Al_2O_3-SiO_2-TiO_2-H_2O-CO_2: representation, estimation, and high temperature extrapolation. Contributions to Mineralogy and Petrology, 89, 168–183.

Brown, N.E. and Navrotsky, A. (1989) Structural, thermodynamic, and kinetic aspects of disordering in the pseudobrookite-type compound karrooite, $MgTi_2O_5$. American Mineralogist, 74, 902–912.

Daniel, C. and Wood, F.S. (1980) Fitting Equations to Data, 2nd ed. Wiley, New York, 458 p.

Ghiorso, M.S. (1990a) Thermodynamic properties of hematite-ilmenite-geikielite solid solutions. Contributions to Mineralogy and Petrology, 104, 645–667.

———(1990b) Application of the Darken equation to mineral solid-solutions with variable degrees of order-disorder. American Mineralogist, 75, 539–543.

Ghiorso, M.S., Evans, B.W., Hirschmann, M.M., and Yang, H. (1995) Thermodynamics of the Amphiboles: I. (Fe^{2+},Mg) Cummingtonite Solid Solutions. American Mineralogist, 80, 502–519.

Hazen, R.M. and Yang, H. (1997) Increased compressibility of pseudobrookite-type $MgTi_2O_5$ caused by cation disorder. Science, 277, 1965–1967.

Hirschmann, M. and Ghiorso, M.S. (1994) Chemical potentials of $NiSi_{0.5}O_2$, $CoSi_{0.5}O_2$, and $MnSi_{0.5}O_2$ in magmatic liquids and applications to olivine-liquid partitioning. Geochimica et Cosmochimica Acta 58, 4109–4126.

Sack, R.O. and Ghiorso, M.S. (1989) Importance of considerations of mixing properties in establishing an internally consistent database: Thermochemistry of minerals in the system Mg_2SiO_4-Fe_2SiO_4-F-SiO_2. Contributions to Mineralogy and Petrology 102, 41–68.

———(1991a) An internally consistent model for the thermodynamic properties of Fe-Mg-titanomagnetite-aluminate spinels Contributions to Mineralogy and Petrology, 106, 474–505.

———(1991b) Chromian spinels as petrogenetic indicators: thermodynamics and petrological applications. American Mineralogist, 76, 827–847.

———(1994a) Thermodynamics of multicomponent pyroxenes: I. Formulation of a general model. Contributions to Mineralogy and Petrology, 116, 277–286.

———(1994b) Thermodynamics of multicomponent pyroxenes: II. Phase relations in the quadrilateral. Contributions to Mineralogy and Petrology, 116, 287–300.

———(1994c) Thermodynamics of multicomponent pyroxenes: III. Calibration of $Fe^{2+}(Mg)_{-1}$, $TiAl(MgSi)_{-1}$, $TiFe^{3+}(MgSi)_{-1}$, $AlFe^{3+}(MgSi)_{-1}$, $NaAl(CaMg)_{-1}$, $Al_2(MgSi)_{-1}$ and $Ca(Mg)_{-1}$ exchange reactions between pyroxenes and silicate melts. Contributions to Mineralogy and Petrology, 118, 271–296.

———(1998) Thermodynamics of feldspathoid solutions. Contributions to Mineralogy and Petrology, 130, 256–274.

Thompson, J.B. Jr. (1969) Chemical reactions in crystals. American Mineralogist, 54, 341–375.

———(1970) Chemical reactions in crystals: Corrections and clarification. American Mineralogist, 55, 528–532.

Waychunas, G.A. (1991) Crystal chemistry of oxides and oxyhydroxides, In Lindsley, D.H., Ed., Oxide Minerals: Petrologic and Magnetic Significance. Mineralogical Society of America, Reviews in Mineralogy, 25, 11–68.

Yang, H. and Hazen, R.M. (1998) Crystal chemistry of cation order-disorder in pseudobrookite-type $MgTi_2O_5$. Journal of Solid State Chemistry, 138, 238–244.

MANUSCRIPT RECEIVED APRIL 13, 1998
MANUSCRIPT ACCEPTED APRIL 24, 1999
PAPER HANDLED BY REBECCA LANGE